Temperature variations in caves induced by atmospheric pressure variations-Part 2: Unveiling hidden thermal signals

Frédéric Perrier, François Bourges, Frédéric Girault, Jean-Louis Le Mouël, Dominique Genty, Bruno Lartiges, Rémi Losno, Stéphane Bonnet

Geosystems and Geoenvironment 2 (2023) 100146

Contents lists available at ScienceDirect

Geosystems and Geoenvironment

journal homepage: www.elsevier.com/locate/geogeo

Temperature variations in caves induced by atmospheric pressure variations—Part 2: Unveiling hidden thermal signals

Frédéric Perrier[a,*], François Bourges[b], Frédéric Girault[a], Jean-Louis Le Mouël[a], Dominique Genty[c], Bruno Lartiges[d], Rémi Losno[a], Stéphane Bonnet[d]

[a] Université Paris Cité, Institut de Physique du Globe de Paris, CNRS, Paris F-75005, France
[b] Géologie Environnement Conseil, 30 rue de la République, Saint-Girons F-09200, France
[c] Environnements et Paléoenvironnements Océaniques et Continentaux, Université de Bordeaux, Pessac Cedex F-33615, France
[d] Université de Toulouse III Paul Sabatier, Géosciences Environnement-Toulouse, Toulouse F-31400, France

ARTICLE INFO

Article history:
Received 6 May 2022
Revised 22 September 2022
Accepted 21 October 2022

Handling Editor: Andrea Festa

Keywords:
Atmospheric pressure
Caves
Natural ventilation
Preservation
Barometric pumping
Critical Zone
Helmholtz resonance

ABSTRACT

In underground cavities, temperature variations of the order of 10^{-3} °C are permanently induced by the variations of atmospheric pressure, even at great depths, with couplings of the order of 0.2 to 20 × 10^{-3} °C/hPa depending on frequency. In the first part of this study, we established the atmospheric pressure to temperature transfer function (TF) as a function of frequency from 8 × 10^{-7} to 8 × 10^{-4} Hz. Here, we use this TF to calculate the expected PIT variations, which, after being subtracted from the observed time-series, provide residual temperature time-series. We calculated such temperature residuals in four natural caves in France: Esparros, Aven d'Orgnac, Pech Merle and Chauvet-Pont d'Arc Caves, the last two containing unique prehistoric wall paintings. Temperature signals, as small as a few 10^{-3} °C, due to human presence, are then conspicuous, with evidence of relaxation longer than several days and long-term cumulative effects. In addition, we observe temperature signals suggesting non-stationary states characterized by several processes which are not necessarily easy to separate, such as transient air currents, due to barometric winds or locally semi-confined convection cells, transient infiltration, or energy dissipation by evaporation-condensation at the rock surface. This background thermal agitation displays a scale-free amplitude spectrum, from 2 × 10^{-5} to 4 × 10^{-4} Hz, of the form $f^{-\alpha}$, with α varying from 0.1 to 0.6 depending on the site. Furthermore, at the Chauvet Cave, a weak but unambiguous peak emerges during some months at a period of about 82.2 ± 0.8 minutes, suggesting a Helmholtz-type resonance. Small but significant temperature signals are therefore detected in underground cavities once the effect of atmospheric pressure variations is corrected for. These signals reveal subtle coupled processes whose knowledge is essential to evaluate preservation strategies and to establish conditions for resilience of underground systems under artificial or natural influence including climate change.

1. Introduction

Underground geosystems, protected from the large meteorological perturbations affecting the ground surface, give unique locations where generic geochemical processes of the Earth, including alteration and precipitation, can be studied with precision in the presence of heat and mass transport (e.g., Genty and Deflandre, 1998; Mangin et al., 1999; Houillon et al., 2017; Bourges et al., 2020). In tunnels and natural caves, signatures of climate change, in particular the long-term evolution of underground temperatures, provide an independent assessment, which is the subject of growing attention (Badino, 2004; Beltrami et al., 2005; Perrier et al., 2005; Dominguez-Villar et al., 2015; Rau et al., 2015). In addition, some underground caves contain precious natural ecosystems (De Freitas et al., 1982), speleothems used for paleoclimate reconstruction (Genty, 2008), or prehistorical paintings (Hoyos et al., 1998; Houillon et al., 2017; Peyraube et al., 2018; Bourges et al., 2014a, 2020). To be able to preserve this heritage, a better understanding of coupled thermo-hydro-chemical and mass processes in caves, which have their specific temperature signals (Morat et al., 1995, 1999), is also an essential prerequisite (e.g., Fernandez et al., 1986; Hoyos et al., 1998; Perrier et al., 2004a; Denis et al., 2005; Bourges et al., 2006; Luetscher et al., 2008; Bourges et al., 2014a).

* Corresponding author.
E-mail address: perrier@ipgp.fr (F. Perrier).

https://doi.org/10.1016/j.geogeo.2022.100146

Competing with geological processes at pluri-annual time-scales, processes at short time-scales, from hourly to seasonal scales, require particular attention when evaluating changes due to human actions. While human intrusion in previously isolated underground systems can cause biological contaminations and degradation (Cañaveras et al., 1999; Martin-Sanchez et al., 2014), one important pending issue remains the primary thermal effect of visitors (Hoyos et al., 1998; Fernandez-Cortes et al., 2011; Saiz-Jimenez et al., 2011). Indeed, the first indication of the presence of one person is, first of all, its metabolic energy, which is equivalent to a heat source of 100 to 140 W (Villar et al., 1984). When a heat source is placed in an air volume, to first order, a turbulent plume is produced above the source, feeding a stratified temperature increase in the rest of the volume (Linden et al., 1990). In the presence of air exchange with an outside reservoir (ventilation), a stationary stratified regime is formed (Linden, 1999), with warm air layers stabilizing near the roof, while the lower part of the volume is not affected, except inside the plume just above the source. This box-filling model is the standard interpretation tool in building ventilation problems (Hunt et al., 2001). In underground locations, this model needs to be modified to incorporate heat exchanges with the encasing rocks (Crouzeix et al., 2006a, 2006b). The resulting modified box-filling model was tested with heating experiments performed in a closed room of an underground quarry in Vincennes near Paris (Crouzeix et al., 2006a, 2006b). These experiments also revealed unexpected features. First, after the interruption of heating, the relaxation phase can be longer than one day, causing cumulative effect after repeated heating sessions. Second, irreversible changes are a possible long-term consequence of the transient heat dissipation (Crouzeix et al., 2003). In addition, long-term fluctuations were observed in the heat plume above the heat source (Crouzeix et al., 2006c) as well as persistent bubbles of warm and cold air (Le Mouël et al., 2016), poorly understood so far. Our knowledge of the effect of heat sources in underground systems appears thus insufficient, even in controlled experiments inside simple geometric volumes such as found in a quarry. In natural caves, with large rooms and complex geometry, the situation is largely unknown (Saiz-Jimenez et al., 2011).

Detecting small temperature signals in natural caves, even in the context of controlled experiments, however, remains difficult (Perrier et al., 2010). Indeed, even at great depth underground (Mangin and D'Hulst, 1996; Perrier et al., 2001), the temperature in the air volume and at the rock surface is always subject to temporal variations due to atmospheric pressure variations (APV). APV produce, at timescales ranging from a few minutes to a few hours, pressure-induced temperature (PIT) variations with peak-to-peak amplitudes larger than 10^{-3} °C (Perrier et al., 2001, 2010, Perrier et al., this issue). These PIT signals have now been detected in numerous underground locations throughout the world, in both natural and artificial underground sites (e.g., Sondag et al., 2003; Perrier et al., 2004a; Bourges et al., 2006; Richon et al., 2009; Šebela and Turk, 2011; Drăguşin et al., 2018; Mejía-Ortíz et al., 2020). To be able to distinguish other thermal processes, it is necessary, first of all, to remove these PIT variations.

In the companion paper (Perrier et al., this issue), we have studied in detail the PIT response functions in four natural caves situated in France, where extensive temperature data are continuously available since 1998: Esparros, Pech Merle, Aven d'Orgnac and Chauvet-Pont d'Arc Caves. The Pech Merle and Chauvet Caves, hosting precious prehistoric paintings, are subject to particular attention (Bourges et al., 2014a, 2014b, 2020). In our four sites, the PIT transfer functions (TFs), precisely measured and interpreted with a thermodynamical model, are now well understood (Perrier et al., this issue).

In the present paper, we use these previously determined TFs to correct the temperature time-series from the PIT variations; we then calculate residual temperature time-series. In addition to anticipated thermal signatures of the presence of visitors, these residuals reveal various types of thermal processes, some of them observed for the first time, which we discuss at each of the four sites. After we have illustrated our capacity to detect small temperature signals, we discuss the various perspectives opened for a better understanding of coupled processes in underground geosystems.

2. Sites and temperature variations induced by atmospheric pressure variations

2.1. Description of the studied caves

The four natural caves selected for this study are located in the South of France (Fig. 1). These sites were described in detail in the companion paper (Perrier et al., this issue). Some aspects relevant for the present work are briefly recalled below.

The Pech Merle Cave, a painted cave (Lorblanchet, 2010), is accessible by an artificial entrance equipped with a double door at an elevation of 284 m above sea level (asl.), and a natural narrow opening at 302 m asl. The two levels (Fig. 1a, b) of the cave system are connected by narrow conduits and a concrete cement staircase. Archaeological remains, including paintings, are only found in the lower level, accessible through an artificial entrance closed by doors. Numerous parts of archaeological value, for example the "Ossuary" Room (O in Fig. 1a, b) are not part of the regular visitors' tour. The upper level, which has largely unexplored narrow extensions, contains red clay fillings ("Red Corridor") and is not included in the visitors' tour since 2007. The total volume of the easily accessible section is estimated to exceed 40,000 m^3.

The Chauvet-Pont d'Arc Cave, famous worldwide because of its exceptional art pieces (Clottes et al., 1995), is located below a limestone cliff above the river gorge (Bourges et al., 2014a, 2014b). The entrance (Fig. 1c), arranged through a narrow conduit above a slope collapse, gives access to reasonably large rooms (Brunel, Bauges and Hillaire Rooms). The remote smaller room ("Remote Room") is not used in the present study. The total volume probably exceeds 40,000 m^3. The access to the Chauvet Cave is restricted to maintenance and archaeological research (Bourges et al., 2014b).

The Gouffre d'Esparros Cave has one main natural entrance giving access to two levels of galleries (Fig. 1e) connected by vertical pits. Visitors access the site by a tunnel into the lower gallery. The "Aragonite Gallery", the most remote part of the lower gallery, is not included in the visitors' pathway. The total volume of the Esparros Cave system is estimated to exceed 30,000 m^3.

The Aven d'Orgnac Cave, located 7 km South-East of the Chauvet Cave (Fig. 1f), has large rooms and a volume of at least 240,000 m^3. Natural air exchange proceeds through a single 15 m vertical pit ("aven") connected to the large De Joly Room (Bourges et al., 2001, 2006).

2.2. Temperature and atmospheric pressure time-series

Continuous measurements of temperature are available for the four sites at several underground locations in the atmosphere and at the rock surface: since 1996 at Aven d'Orgnac and Esparros Caves, since 1997 at the Chauvet Cave and since 1998 at the Pech Merle Cave. These data were complemented by data from temporary experiments performed between 2015 and 2018. In the present study, the sensors are labelled as in the companion paper (Perrier et al., this issue). The first letter ("T" for temperature, "p" for atmospheric pressure) indicates the type of sensor. The following two letters ("Es" for Esparros, "Pm" for Pech Merle, "Ch" for Chauvet and "Or" for Aven d'Orgnac Caves) refer to the cave. After the site name, the capital letter indicates the location within the

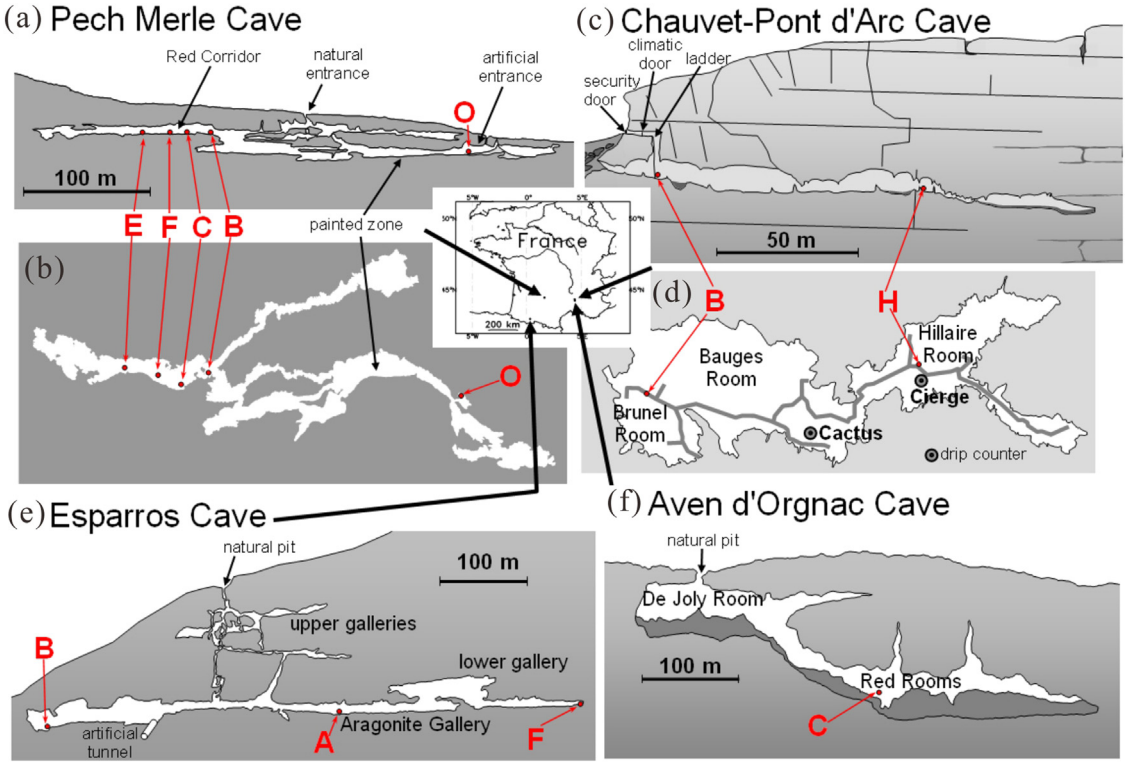

Fig. 1. Location of Esparros, Pech Merle, Chauvet-Pont d'Arc and Aven d'Orgnac Caves. A simplified cross-section of each cave shows the positions of sensors used in the present study. The simplified cross-sections are drawn from available topographic data. In addition, simplified map layouts are shown for the two caves with prehistorical artwork and human remains: Pech Merle (Fig. 1a, b) and Chauvet (Fig. 1c, d) Caves. The location of the measurement points is indicated with capital letters in red.

site, as given in Fig. 1. The final index indicates whether the measurement is in air ("a") or at the rock surface ("r"). For example, label "$TEsF_a$" refers to the temperature measurement in the atmosphere of the Esparros Cave at the end of the Aragonite section (location F, Fig. 1e).

Two types of thermometers were used in this study (see the companion paper Perrier et al., this issue). For long records with a sampling interval of 15 min, available over more than 20 years at the four sites, Pt100 thermometers were used, with a noise level of the order of 10^{-3} °C. For temporary experiments with a duration from a few months to a few years, autonomous Seabird™ recorders (SB) were used, which utilize a high sensitivity thermistor. This second type of sensor allows lower noise levels, of the order of 2 to 3 $\times$ 10^{-4} °C (see below).

In the present study, we used data collected at some of the monitoring points (see locations in Fig. 1) studied in the companion paper (Perrier et al., this issue). As an example, complementing time-series shown in the companion paper, time-series of temperature and atmospheric pressure collected at various locations in the Esparros Cave (Fig. 2) illustrate the main properties of the PIT. At point A (Aragonite Gallery), the air temperature shows conspicuous PIT signals, with a peak-to-peak amplitude of 90 $\times$ 10^{-3} °C over the considered time period (Fig. 2a), caused by APV having a peak-to-peak amplitude of 15 hPa. PIT signals at the rock surface are smaller, but visible, with a corresponding peak-to-peak amplitude of 15 $\times$ 10^{-3} °C (Fig. 2a). PIT variations similar to the variations of $TEsA_a$ are observed simultaneously (Fig. 2b) at the two other points $TEsF_a$ and $TEsB_a$, located at a distance of 270 m and 220 m from point A, respectively. The peak-to-peak amplitudes at these points are 10 $\times$ 10^{-3} °C and 21 $\times$ 10^{-3} °C, respectively. Large spatial variations of the PIT amplitude, already observed previously at other locations (Perrier et al., 2010), were observed in the four considered caves.

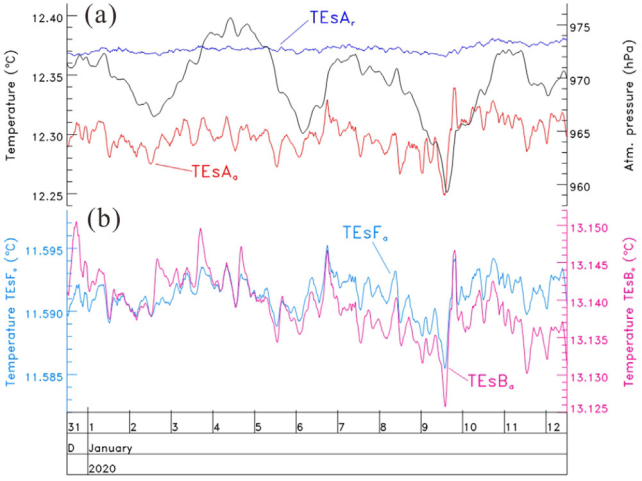

Fig. 2. Selected time-series at the Esparros Cave (see location of sensors in Fig. 1e): (a) air ($TEsA_a$) and rock surface ($TEsA_r$) temperatures in the Aragonite Gallery, together with atmospheric pressure (in black, right-hand scale); (b) air temperature at points F ($TEsF_a$, end of the Aragonite Gallery) and B ($TEsB_a$, above the lake). The temperature scale for $TEsB_a$ is given on the right-hand side. The time-series $TEsA_a$ and $TEsA_r$ (sampling interval 15 min), as well as the time-series $TEsF_a$ and $TEsB_a$ (sampling interval 2 min) are averaged with a moving window of 2 h width.

2.3. Determination and modelling of the PIT transfer functions

The TFs were calculated in the frequency domain using a robust algorithm, as elaborated in the companion paper (Perrier et al., this issue). The pressure to air temperature TF, evaluated from 8 $\times$ 10^{-7} to 8 $\times$ 10^{-4} Hz, strongly depends on frequency. Depending on the considered point in a given cave

(Perrier et al., this issue), its modulus, which varies from 2 to 14×10^{-3} °C/hPa at the barometric tide S2 (12 h), rises from 0.2 to 1×10^{-3} °C/hPa at low frequency and from 11 to 45×10^{-3}°C/hPa at high frequency. The observed spatial variations of the PIT TF in these caves are compatible with previous detailed studies at the Vincennes Quarry near Paris (Perrier et al., 2010) where the distance to the nearest rock surface was found to be an important factor. While the TFs displayed remarkable long-term stability at all sites over durations larger than 5 years at the Chauvet Cave and over more than 15 years at the Esparros Cave, significant seasonal variations of the order of 20 to 40% are observed at most locations.

The air to rock surface temperature TF was calculated for the first time at selected points at Esparros, Chauvet and Pech Merle Caves (Perrier et al., this issue). This TF shows a gentle variation with frequency. Its modulus decreases from about 0.6 at low frequency (8×10^{-7} Hz) to a limit of about 0.1 to 0.4, depending on the considered point, at high frequency (8×10^{-4} Hz).

The observed TFs were accounted for by an analytical model (Perrier et al., this issue). In this model, the atmospheric pressure to air temperature ($\hat{T}/\hat{p}$) and the air to rock temperature ($\hat{T}_r/\hat{T}_a$) TFs have expressions depending on frequency f and on three free parameters, whose numerical values have been determined for each of the considered monitoring points. The analytical forms of the TFs with the determined values of the parameters are used in the following.

2.4. Subtraction of the PIT variations

In the present paper, we focus on the temperature residuals after PIT subtraction (PITS). The principle of PITS is described as follows (Perrier et al., 2001, 2010). For air temperature PITS, the atmospheric pressure time-series p_i is transformed into the Fourier domain $\hat{p}_j$, multiplied by the theoretical TF $\hat{T}_a/\hat{p}(f_j)$ versus frequency; the result $\hat{T}_a/\hat{p}(f_j) \times \hat{p}_j$ is then transformed back into the time domain by inverse Fourier transform to obtain the calculated theoretical time-series $T_{a,i}^{PIT}$. The residual R_a is then defined as the difference between the measured and the calculated time-series: $R_a = T_{a,i}^{meas} - T_{a,i}^{PIT}$.

For rock surface temperature, the air temperature time-series T_{ai} is transformed into the Fourier domain $\widehat{T_a}_j$, multiplied by the theoretical TF $\hat{T}_r/\hat{T}_a(f_j)$ versus frequency; the result $\hat{T}_r/\hat{T}_a \times \widehat{T_a}_j$ is then transformed back into the time domain by inverse Fourier transform to calculate theoretical time-series $T_{r,i}^{PIT}$. The residual R_r is then defined as the difference between the measured and the calculated time-series: $R_r = T_{r,i}^{meas} - T_{r,i}^{PIT}$. In the following, the residual for a given variable is labelled with "R" followed by the name of the variable.

On average, the process is efficient, as will be shown in the examples below. In particular, no significant correlation with atmospheric pressure (coherency smaller than a few % over the whole frequency range) is observed for the residuals. However, it is important to remember that the TFs used in the PITS are average and stationary TFs, which does introduce some intrinsic limitations, as will arise when studying the observed residuals in detail.

3. Residual temperature variations in caves

In the following, we present various observations for each cave, and collect the properties of the temperature residuals after PITS. These observations are then synthetized and analysed jointly.

3.1. Temperature residuals after PITS at the Esparros Cave

A first typical example of the PITS process is shown in the case of the Esparros Cave (Fig. 3). The calculated time-series (in blue in Fig. 3a) appears similar to the observed time-series (in red). The calculation of PIT time-series thus offers an adequate representation of the observed PIT. The inferred residual, shown in green in Fig. 3b, does not show any further correlation with atmospheric pressure, with a coherency in this instance smaller than 0.2 over the whole frequency range for the considered period from September, 2005 to September, 2008.

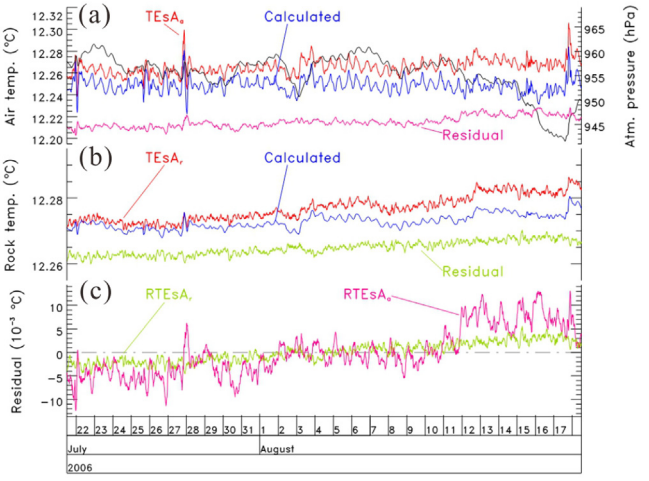

Fig. 3. Air temperature time-series from the Esparros Cave (Aragonite Gallery): (a) air temperature (TEsA$_a$), (b) surface rock temperature (TEsA$_r$) and (c) residual time-series. The measured time-series in a) and b) are shown in red, the calculated PIT time-series in blue, and the residual, defined as the difference between the measured and the calculated time-series, in purple (RTEsA$_a$) and in green (RTEsA$_r$). The calculated and residual time-series are shifted arbitrarily for clarity. The atmospheric pressure time-series (in black) is shown in (a) with the scale given on the right-hand side. The time-series are averaged with a moving window of 2 h width.

The residuals (Fig. 3c) show only small variations, with peak-to-peak amplitudes of 25×10^{-3} °C and 10×10^{-3} °C over the range shown in Fig. 3, for RTEsA$_a$ and RTEsA$_r$, respectively. The RTEsA$_r$ residual shows a linear increasing trend, which accounts for half of the observed variation, with a standard deviation of 2.7×10^{-3} °C, compared with 5.7×10^{-3} °C, for RTEsA$_a$. Indeed, conspicuous temperature variations are observed in the RTEsA$_a$ residual, especially after August 11, 2006, with an overall step of about $+5 \times 10^{-3}$ °C, while the standard deviation of RTEsA$_a$ (4×10^{-3} °C) is smaller before this date.

The RTEsA$_a$ signals, thus evidenced, tend to have typical periods from a few hours to a few days. The smaller RTEsA$_r$ high-frequency signals could be instrumental noise. Incidentally, they also demonstrate that the larger RTEsA$_a$ signals, then, cannot be attributed to such instrumental noise; a physical thermal source must be present in the atmosphere, with little effect on the rock surface. At this stage, transient air currents can be proposed already as a plausible explanation (see discussion below).

Amplitude spectra (Fig. 4) provide a global view on the PITS process and present overall statistical properties of the RTEsA$_a$ and RTEsA$_r$ residuals. The measured time-series are characterized by the dominance of the S2 oscillation, which results from PIT due to the S2 barometric tide, which stands out in the spectrum of atmospheric pressure (Fig. 4). After PITS, the amplitude spectrum of RTEsA$_a$ is reduced overall by about a factor of two over the whole frequency range compared with the amplitude spectrum of TEsA$_a$, and the S2 peak is reduced by at least a factor of 3 and becomes smaller than the S1 peak. The overall reduction of the spectrum from TEsA$_r$ to RTEsA$_r$ is smaller, except for the S2 peak, which is almost completely eliminated in RTEsA$_r$. Thus, the temperature residuals, unlike the original time-series, are characterized by S1 dominance, indicating diurnal processes, which can be of natural or artificial origin.

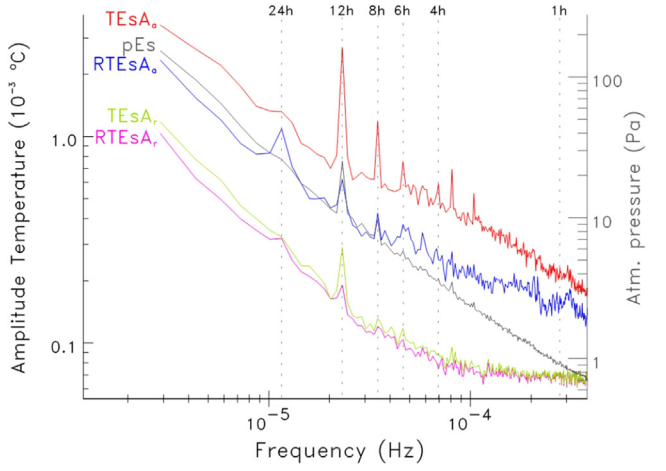

Fig. 4. Amplitude spectra versus frequency of temperature time-series in the Aragonite Gallery at the Esparros Cave: atmospheric pressure (in black, right-hand scale), measured air temperature $TEsA_a$, residual air temperature $RTEsA_a$ after PITS, measured rock surface temperature $TEsA_r$ and residual air temperature $RTEsA_r$ after PITS. Spectra are calculated by stacking 13 portions of 768 data points with 15 min sampling interval.

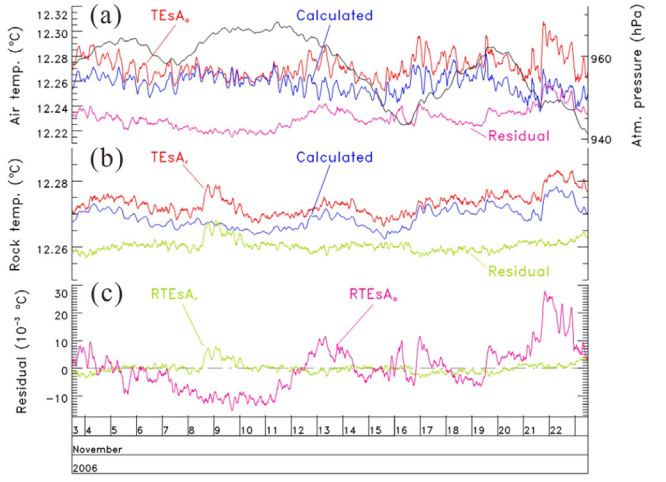

Fig. 5. Air temperature time-series from the Esparros Cave (Aragonite Gallery): (a) air temperature ($TEsA_a$), (b) surface rock temperature ($TEsA_r$) and (c) residual time-series. The measured time-series in (a) and (b) are shown in red, the calculated PIT time-series in blue, and the residual, defined as the difference between the measured and the calculated time-series, in purple ($RTEsA_a$) and in green ($RTEsA_r$). The calculated and residual time-series are shifted arbitrarily for clarity. The atmospheric pressure time-series (in black) is shown (a) with the scale given on the right-hand side. The time-series are averaged with a moving window of 2 h width.

Other types of transient changes of the residuals can be observed by detailed inspection of the time-series (Fig. 5), while the large PIT variations are adequately corrected for (Fig. 5a, b). First, $RTEsA_a$ signals can be of larger amplitude than those observed in Fig. 3, reaching more than 20 $\times$ 10^{-3} °C peak-to-peak, and of a duration of several days (Fig. 5c), with transient periods of signals as large as 15 $\times$ 10^{-3} °C and of shorter durations, for example on November 22, 2006 (Fig. 5c). The $RTEsA_r$ signal (Fig. 5b, c) shows a small but unequivocal transient positive variation on November 8-9, 2006, with a peak amplitude of 7 $\times$ 10^{-3} °C, without relationship to the $RTEsA_a$ signal, decaying in about three days. Such transient, involving only the rock surface, could result from a transient liquid water thin film flowing at the sensor location, or from water vapour condensation, not necessarily related to air motion.

In some cases (Fig. 6), the reason for temperature transients is clear, e.g., the presence of visitors in the cavity. While the Aragonite Gallery is not part of the touristic visit, some occasional, strictly regulated, human presence is necessary for maintenance and cave survey. One adult human produces a metabolic heat production of about 140 W, which results in a heating signal easily detectable in stable environments (Villar et al., 1984; Crouzeix et al., 2003, 2006a, 2006b). While the effect is not easy to detect in the raw temperature time-series (Fig. 6a), except for $TEsA_r$, it becomes apparent when looking at the residuals (Fig. 6b). The peak amplitude in this case is large; it reaches 51 $\times$ 10^{-3} °C and 20 $\times$ 10^{-3} °C in $RTEsA_a$ and $RTEsA_r$, respectively. The presence of the maintenance team is detected as well at the most remote point F of the Aragonite Gallery and the regular visitors are observed at point B above the lake (Fig. 1e), with a similar amplitude of 11 $\times$ 10^{-3} °C in both cases. At point F, where the amplitude of natural signals is reduced compared with $TEsA_a$, a transient heating effect as small as 10^{-3} °C could be easily detected after PITS.

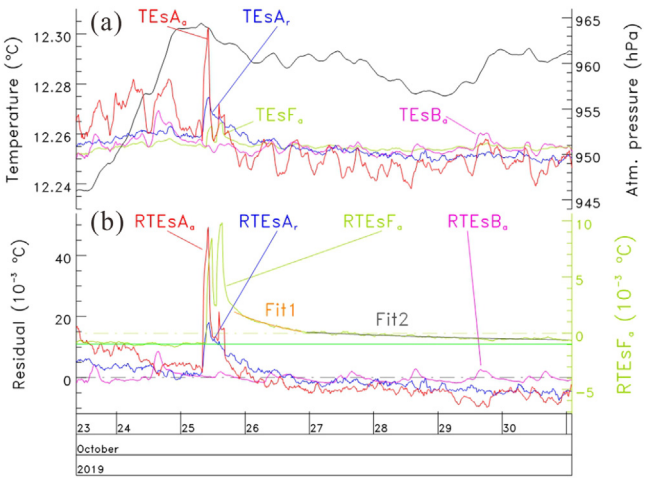

Fig. 6. Measured temperature time-series and residuals recorded at points A, F and B of the Esparros Cave. (a) Measured temperature time-series and atmospheric pressure (in black, scale on the right-hand side). The mean temperatures of $TEsA_r$, $TEsF_a$ and $TEsB_a$ are shifted to be the same as the mean temperature of $TEsA_a$ during the displayed time period. (b) Residuals after PITS. A separate scale is used for $RTEsF_a$, given on the right-hand side. The time-series $TEsA_a$, $TEsA_r$, $RTEsA_a$ and $RTEsA_r$ (sampling interval 15 min), as well as the time-series $TEsF_a$, $TEsB_a$, $RTEsF_a$ and $RTEsB_a$ (sampling interval 2 min) are averaged with a moving window of 2 h width.

The thermal relaxation after transient heating (Fig. 6a) deserves some attention. As already mentioned above in the introduction, it shows two phases (Crouzeix et al., 2003, 2006a, 2006b): a rapid relaxation of about 18 to 25 minutes, which corresponds to the characteristic thermal exchange time τ (Crouzeix et al., 2006a, 2006b; Perrier et al., this issue) and a long non-exponential relaxation due to heat diffusion in the rock, which damps the relaxation in the atmosphere. As indicated in Fig. 6b, this long relaxation can last several days and can be evolutive. At point F, from 12 hours to 36 hours after the heating, an exponential fit (Fit 1, orange curve) gives a decay constant of 26.6 $\pm$ 0.1 hours, while over the following four days (Fit 2, grey curve) the decay constant becomes 3.90 $\pm$ 0.02 days. The small temperature excess remaining after 5 days, of the order of 10^{-4} °C, cannot be distinguished from a slow variation of the base-line.

In the absence of maintenance in the Aragonite Gallery, it is interesting to compare the various residuals available at various points of the cavity (Fig. 7), during an episode of reasonably small atmospheric pressure variations, dominated by the S2 barometric tide (Fig. 7a). No S2 variation remains after PIT subtraction (Fig. 7b), but the residuals display significant peak-to-peak variations, ranging, after subtraction of the long-term trend during the considered period, from 1.3 $\times$ 10^{-3} °C for $RTEsF_a$, to 8.3 $\times$ 10^{-3} °C

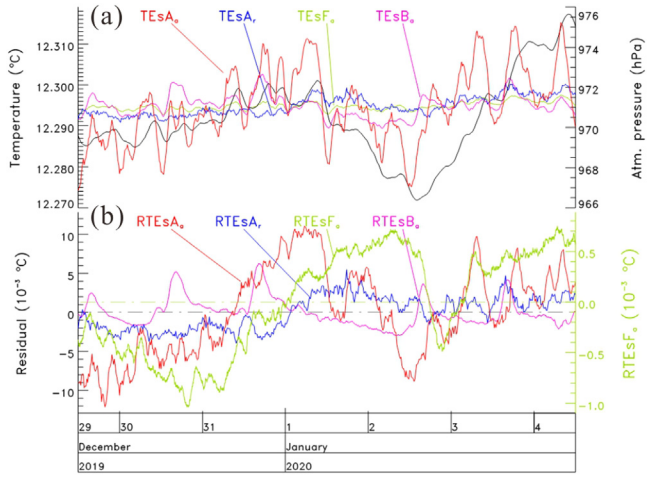

Fig. 7. Measured temperature time-series and residuals recorded at points A, F and B of the Esparros Cave. (a) Measured temperature time-series and atmospheric pressure (in black, scale on the right-hand side). The mean temperatures of $TEsA_r$, $TEsF_a$ and $TEsB_a$ are shifted to be the same as the mean temperature of $TEsA_a$ during the displayed time period. (b) Residuals after PITS. A separate scale is used for $RTEsF_a$, given on the right-hand side. The time-series $TEsA_a$, $TEsA_r$, $RTEsA_a$ and $RTEsA_r$ (sampling interval 15 min), as well as the time-series $TEsF_a$, $TEsB_a$, $RTEsF_a$ and $RTEsB_a$ (sampling interval 2 min) are averaged with a moving window of 2 h width.

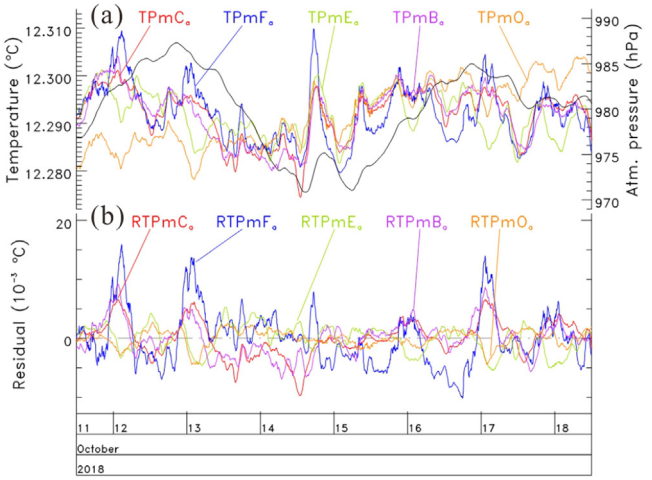

Fig. 8. Measured temperature time-series and residuals recorded at selected points of the Pech Merle Cave. (a) Measured temperature time-series and atmospheric pressure (in black, scale on the right-hand side). The mean temperatures of time-series are shifted to be the same as the mean temperature of $TPmC_a$ during the displayed time period. (b) Residuals after PITS. The time-series (sampling interval 2 min) are averaged with a moving window of 48 samples width.

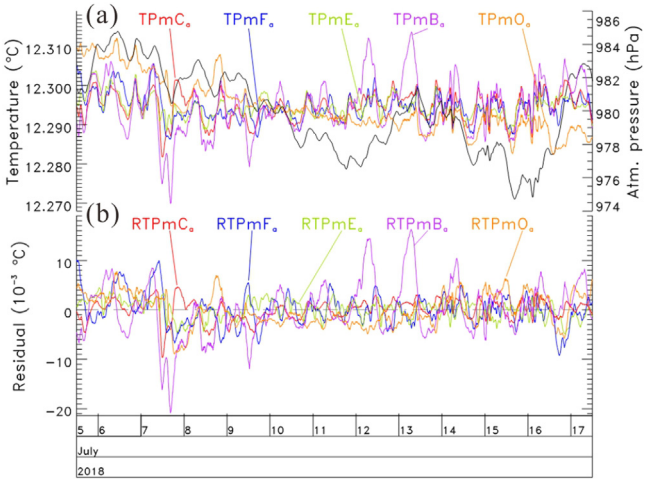

Fig. 9. Measured temperature time-series and residuals recorded at selected points of the Pech Merle Cave. (a) Measured temperature time-series and atmospheric pressure (in black, scale on the right-hand side). The mean temperatures of time-series are shifted to be the same as the mean temperature of $TPmC_a$ during the displayed time period. (b) Residuals after PITS. The time-series (sampling interval 2 min) are averaged with a moving window of 36 samples width.

and 22×10^{-3} °C for $RTEsA_r$ and $RTEsA_a$, respectively. Daily transients of 5×10^{-3} °C amplitude in $RTEsB_a$ are due to the regular touristic visits, as discussed above. No such transient took place on January 1st, 2020, when the cave was closed. Unlike the maintenance visits shown in Fig. 6, the regular tours do not enter the Aragonite Gallery, and therefore do not produce heating transients at point A. In the instance considered in Fig. 7, the residual signals, with dominating periods of a few hours, are the largest in $RTEsA_a$, but quite significant in $RTEsA_r$. While the amplitude is smaller at point F (right-hand scale in Fig. 7b), variations can be observed because of the enhanced stability at that location, for example the about 14-hour-long transient on January 2nd, 2020. No obvious relationship between the various signals can be noticed, but these points A, F and B may be located too far away from each other, in different air current systems. When searching for correlations between residuals, it is better to focus on sites with several sensors in the same gallery located closer to each other. This is possible in the Red Corridor of the Pech Merle Cave.

3.2. Temperature residuals after PITS at the Pech Merle Cave

At the Pech Merle Cave, the calculated PIT time-series, studied here at points C, F, E, B and O (Fig 1b) are of remarkable accuracy, as in the Esparros Cave (Fig. 8a); the residuals are small, with standard deviations, over the period displayed in Fig. 8, of 3.3×10^{-3} °C, 7.6×10^{-3} °C, 2.6×10^{-3} °C, 3.6×10^{-3} °C and 6.3×10^{-3} °C, respectively. No visitor-induced signal was observed during this considered period of October 2018, but such signal, when present, is distinctly observed in the residuals in the Pech Merle Cave as well (Supplementary Data, Fig. S1), followed by its now familiar long relaxation phase. The amplitude spectra in the Pech Merle Cave are characterized, after subtraction, by almost complete elimination of the S2 peak, and replacement of S2 dominance in the raw time-series by S1 dominance over S2 in the residuals (Supplementary Data, Fig. S2). In fact, in the unvisited parts of the Pech Merle Cave, the S1 peak and its harmonics are almost completely eliminated as well. Compared with the amplitude of the measured temperature, the amplitude of the continuum residual spectrum is reduced by a factor larger than 8 at frequencies smaller than 10^{-5} Hz, and larger than 2 at frequencies smaller than 10^{-4} Hz (Supplementary Data, Fig. S2).

Interesting signals emerge in the residuals (Fig. 8b), in particular nocturnal transient signals from October 11 to October 13, simultaneously detected by several sensors. Thus, in this system, a long-distance coherence of the transient signals in the atmosphere is observed, with opposite phase and smaller amplitude at points E and O. These transient signals are particularly significant as the large pressure variations occurring from October 14 to October 15, and the associated large S2 oscillations are properly calculated and eliminated from the residuals. In that case, a transient change in the PIT response can thus be ruled out, and the signals then reveal slow variations of the transport processes in the atmosphere.

In addition, at some other times, non-synchronous transient signals can be observed at various points (Fig. 9). The negative bay-like signal from July 7 to 9 offers a particularly interesting instance of a slowly propagating process started in the middle of the Red

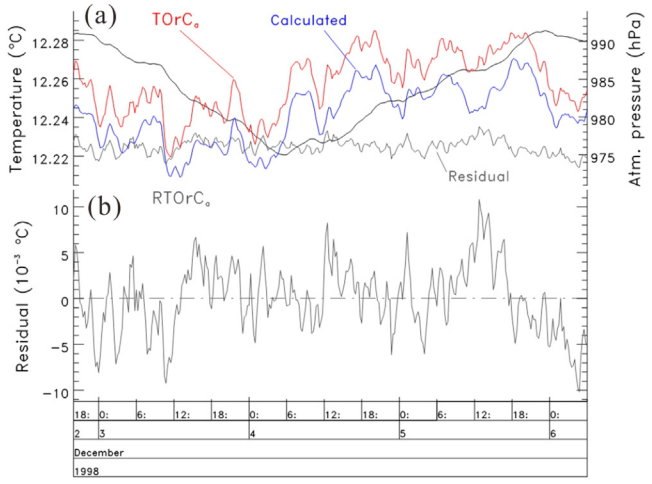

Fig. 10. Temperature time-series from the Aven d'Orgnac Cave. (a) Measured air temperature time-series (TOrC$_a$ in red), calculated time-series (in blue), and residuals defined as the difference between the measured and the calculated time-series (in grey). The calculated and residuals time-series are shifted for clarity. The atmospheric pressure time-series is shown (in black) with the scale given on the right-hand side. (b) Time-series of the residuals are shown with an enlarged scale. The time-series (sampling interval 15 min) are averaged with a moving window of 1 h width.

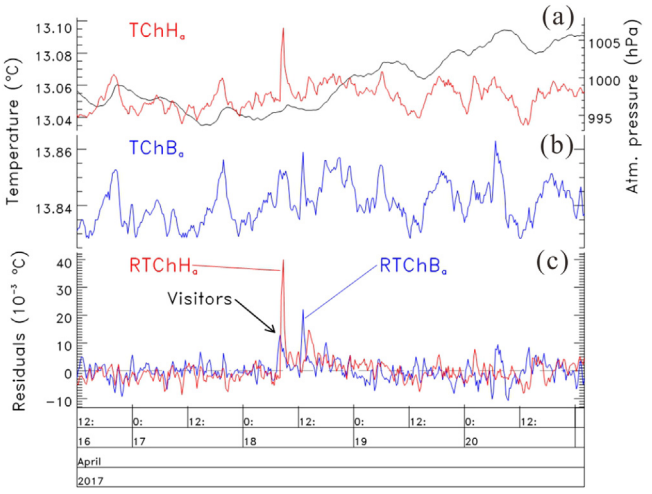

Fig. 11. Air temperature time-series from the Chauvet Cave: (a) measured temperature in the Hillaire Room (TChH$_a$ in red) with the atmospheric pressure time-series (in black) shown with the scale given on the right hand side, (b) measured temperature in the Brunel Room (TChB$_a$ in blue) and (c) corresponding residuals time-series after PITS. The time-series (sampling interval 15 min) are averaged with a moving window of 30 min width.

Corridor, and moving simultaneously to the end part on the one hand, and to the natural entrance and lower part of the cave on the other hand. Furthermore, after July 12, a daily signal emerges at point B, decaying slowly during the following days. This slow signal cannot be directly attributed to the presence of visitors and in any case does not display the signature of human heating. However, it could be an indirect effect of the presence of visitor groups in the lower part of the cave, which causes the manipulation of the doors and the artificial initiation of air currents from the natural entrance. Therefore, residuals at the Pech Merle Cave show a variety of transients in the residuals, which, after knowing that they can possibly occur, can be searched at other locations.

3.3. Temperature residuals after PITS at the Aven d'Orgnac Cave

In the Aven d'Orgnac Cave, the PITS is also performing remarkably (Fig. 10a). The thermal effect of visitor groups, which is of the same order of magnitude as the PIT variations, is seen after PITS (Supplementary Data, Fig. S3), with a peak amplitude of 40×10^{-3} °C associated with repeated groups of about 20 persons. The effect is particularly interesting in this case because the sensor is located more than 25 m away from the visitors' position (see Fig. 1f), in a large room (height larger than 20 m), about 13 m lower. This is thus analogous to the situation of sensor B above the lake in the Esparros Cave, below the visitors' balcony (Fig. 1e). In addition, the sensor is not visible from the visitors' location, which rules out any thermal effect due to direct radiation. In this particular case, the main heating effect may be due to the projectors which are switched on during the visit. This lighting system was only recently replaced by low dissipation lights.

In the absence of visitors, residual signals remain in the RTOrC$_a$ residual (Fig. 10b). With a standard deviation of 5×10^{-3} °C, which is much larger than the possible instrumental noise limit inferred from the sensors at the rock surface in the Esparros Cave (see above), these signals do not display a larger amplitude than those observed in Esparros or Pech Merle Caves. This suggests that the significantly larger volume of the cavity at Aven d'Orgnac Cave does not lead to signals of larger amplitude. Following this line of thought, it is interesting to study the temperature residuals in the Chauvet Cave, where the volumes of the cavities are much smaller.

3.4. Temperature residuals after PITS at the Chauvet Cave

In the Chauvet Cave, human presence is severely restricted to avoid environmental changes and is subject to safety protocols to prevent accidental contaminations to the prehistoric artwork. Given the smaller volumes and the smaller distances to the sensors, the thermal effect of visitors is larger than 40×10^{-3} °C for two visitors (maintenance team) in the Hillaire Room (Fig. 11). While the peak effect is visible in the raw temperature TChH$_a$ (Fig. 11a), the complete development of the thermal perturbation down to 5×10^{-3} °C, can only be seen in the RTChH$_a$ residual (Fig. 11b). These visitors only pass through the Brunel Room (Fig. 1d), and the associated elusive thermal signature is completely hidden below the PIT of TChB$_a$ (Fig. 11a). Nevertheless, an unambiguous signal with amplitude 10×10^{-3} °C is revealed in the RTChB$_a$ residual (Fig. 11b), about 45 minutes before RTChH$_a$ residual. Thus, to monitor the thermal signature of visitors for preservation, PITS is mandatory and is adequate to extract the relevant signals with sufficient accuracy.

The thermal effects of human presence in the Chauvet Cave are obviously larger during the archaeological surveys, which can involve more than ten people at a given time. Such repeated sessions take place once or twice per year maximum. Even during such periods, the thermal perturbations emerge distinctly only after PITS (Fig. 12). When the visits are repeated, the cumulated increase of temperature is striking. As observed before May 30 or before June 6, 2016, the thermal relaxation after one day with human presence is longer than several days, as established in the Esparros Cave or the Vincennes Quarry. Thus, when visits take place during several consecutive days, for example from May 10 to 15, 2016 in Fig. 12, then the return to the thermal equilibrium is incomplete and the effect of the current visit is added to the thermal remnant of the previous day. The cumulated effect of several days of survey can be larger than 20×10^{-3} °C and a temperature excess of 10×10^{-3} °C is still visible three weeks after the end of the campaign (Fig. 12). This cumulative effect, in part due to the diffusive relaxation contribution mentioned above, was measured precisely in experiments carried out at the Vincennes Quarry (Crouzeix et al., 2006b). It was concluded that the temperature change due to a sequence of heatings might be irreversible (Crouzeix et al., 2003). It is premature to state whether this conclusion could apply in the case of the

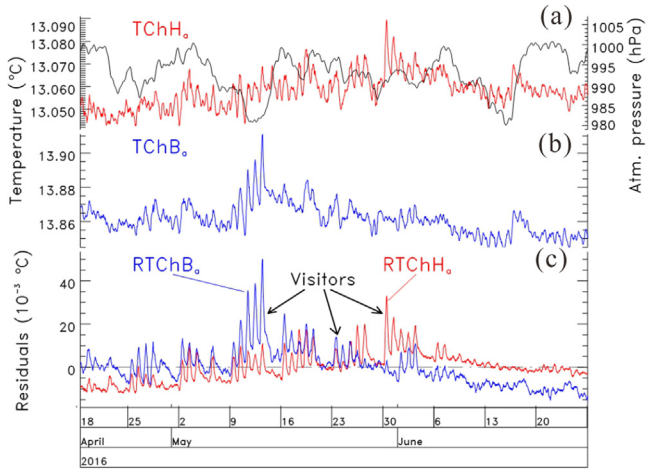

Fig. 12. Air temperature time-series from the Chauvet Cave: (a) measured temperature in the Hillaire Room (TChH$_a$ in red) with the atmospheric pressure time-series (in black) shown with the scale given on the right hand side, (b) measured temperature in the Brunel Room (TChB$_a$ in blue) and (c) corresponding residuals time-series after PITS. The time-series (sampling interval 15 min) are averaged with a moving window of 8 hours width.

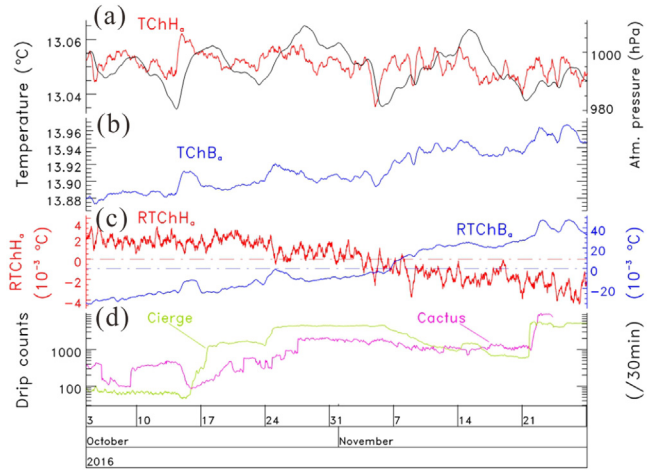

Fig. 13. Air temperature and drip counts time-series from the Chauvet Cave: (a) measured temperature in the Hillaire Room (TChH$_a$ in red) with the atmospheric pressure time-series (in black) shown with the scale given on the right hand side, (b) measured temperature in the Brunel Room (TChB$_a$ in blue), (c) corresponding residuals time-series after PITS and (d) drip counts, expressed in drops per 30 min. The temperature time-series (sampling interval 15 min) are averaged with a moving window of 12 h width. The drip time-series (sampling interval 30 min) are averaged with a moving window of 1 h width.

Chauvet Cave. Nevertheless, a reasonable recommendation would be to restrict the archaeological work in the cave to one day per week maximum, so that the thermal equilibrium could be completely restored before the next visit. This may cause, however, unmanageable logistic issues. In general, it should nevertheless be required that no remnant thermal effects should be observed to the resolution limit of the sensors and the detection capacity of the temperature residuals.

In the absence of visitors, as in the other sites, signals are observed in the temperature residuals in the Chauvet Cave. In this case, however, some signals could be further studied thanks to additional data (Bourges et al., 2020). Indeed, transient variations as large as 10×10^{-3} °C, on top of a regular temperature increase, emerge in the RTChB$_a$ residual during some particular periods (Fig. 13), while the signals on the RTChH$_a$ residual, with a standard deviation of 1.8×10^{-3} °C, is only larger than the instrumental noise of about 10^{-3} °C. The transient increases in RTChB$_a$ coincide with large increases in the drip counts recorded in the Cierge drip counter, and, possibly, with transient decreases in the Cactus drip counter as well (Fig. 13d). Thus, these temperature signals could be interpreted as transient condensation events resulting from over saturation of the cavity atmosphere.

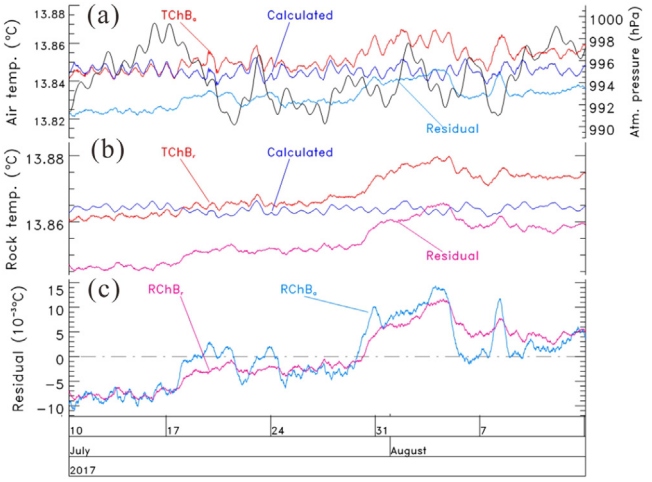

Fig. 14. Temperature time-series in the atmosphere of the Brunel Room of the Chauvet Cave: (a) air temperature (TChB$_a$), (b) surface rock temperature (TChB$_r$) and (c) residual time-series. The measured time-series in (a) and (b) are shown in red, the calculated PIT time-series in blue, and the residual, defined as the difference between the measured and the calculated time-series, in green. The calculated and residual time-series are shifted arbitrarily for clarity. The atmospheric pressure time-series (in black) is shown (a) with the scale given on the right-hand side. The time-series (15 min sampling interval) are averaged with a moving window of 12 h width.

However, variations such as shown in Fig. 13, suggesting correlations between temperature transients and drip events, are rare. Most of the time, no convincing relation can be evidenced at timescales shorter than a day between temperature transients observed in the residuals, drip counts or other parameters available in the cave. In the Brunel Room, nevertheless, it is possible to compare the RTChB$_a$ and RTChB$_r$ residuals, as the atmosphere to rock temperature TF could be determined at that location (Perrier et al., this issue). The calculation of PIT variations can then be performed to a high degree of accuracy for both TChB$_a$ and TChB$_r$ (Supplementary Data, Fig. S4). Transient signals then can be observed simultaneously in the atmosphere and at the rock surface of the Brunel Room (Fig. 14). These positive bay-like signals, with amplitude from 6 to 8 $\times$ 10^{-3} °C and of a duration of several days, coincide approximately in RTChB$_a$ and RTChB$_r$ time-series (Fig. 14c). As air current effects, described above, give a dominating response in the atmosphere, the source here must be in the rock mass. The intriguing aspect of these signals is the fast relaxation, shorter than one day, excluding a control by heat diffusion. One possibility in this case is the presence of thin water films, able to modify the thermal response at the rock surface, but otherwise difficult to detect.

4. Residual temperature signals: Overview and discussion

4.1. Overview of temperature transients: Global versus local air motions and thermodynamics

From the previous observations at our four sites, we can state that PITS, not only performs with sufficient accuracy in all studied circumstances, but appears as an essential tool to unveil hidden thermal signals. Indeed, almost none of the signals discussed above could have been evidenced without PITS.

In all cases, the presence of visitors in the cavities is unambiguously detected from the residuals. When the local cavity volumes are relatively small (compared for example with the De Joly Room of the Aven d'Orgnac Cave), as in the remote parts of the Esparros or Chauvet Caves, the standard box-filling model (Linden et al., 1990; Crouzeix et al., 2006a) is probably compatible with the observations. In this model, a heat plume is generated above a heat source, which rises and feeds a warm layer at the roof of the cavity, with a transition zone slowly coming down, reaching an equilibrium level in the presence of air exchange (Crouzeix et al., 2006a, 2006b). However, in this case, the thermal visitor signals observed below the balcony in the Esparros Cave (point B) and in the Aven d'Orgnac Cave are difficult to accommodate with this model. Indeed, the temperature increase is observed at a significantly lower level (−5 m at least) below the visitors' path level, in a large room, and far away in the case of the Aven d'Orgnac Cave. In this case, the observations from the temperature residuals, rather, suggest that the presence of the visitor group initiates a large-scale convection cell in the cavity, reaching the upper roof surfaces, then returning by sweeping the floor levels and closing back the convection loop at the visitors' level. Such a scenario is incompatible with a filling-box type model. The current data, however, are insufficient to confirm such a process and additional dedicated experiments are needed.

In the absence of visitors, natural signals dominate the air temperature residuals. Some signals seem to be permanently observed, while larger transient signals, sometimes observed simultaneously at different locations of the same cave system, only appeared at specific moments. The detected signals are of various shapes, sometimes bipolar wavelike damped oscillations and sometime discrete jumps (Fig. 3), similar to sudden changes observed in the access pit of the Vincennes Quarry and interpreted as transitions between several possible quasi-stable thermodynamic states (Perrier and Le Mouël, 2016).

While some transient changes of large-scale convection cells are possible, for example in the Pech Merle Cave, the similarity of the amplitude of air temperature residuals at the various locations and in the various caves rather suggests changes in local convection cells, typically with a scale of a few meters. In addition, the non-synchronous signals observed in the Red Corridor of the Pech Merle Cave suggest the presence of slowly propagating air currents, or convection slowly adjusting cells from place to place. Laminar air currents or plumes slowly creeping on the floor or the roof of tunnels are not ruled out. Turbulent motions are probably not required, depending on the considered spatial scale, when velocities drop below a few meters per hour.

Beyond processes taking place in the atmosphere, processes involving the rock mass are observed when combining the atmosphere and rock surface residuals. In one instance, in the Chauvet Cave, a transient infiltration could be proposed as a likely cause (Fig. 13). However, in most cases, the source of the transient temperature change remains unclear. Sometimes, transients are observed only with the rock surface residual (Fig. 5), thus suggesting evaporation-condensation processes. While thin films can be considered to play a potentially important role, they remain an unconfirmed hypothesis at this stage.

4.2. Overview of amplitude spectra of the residuals after PITS

Complementing the examination of the time-series, it is interesting to study the average structure of the temperature residuals using their amplitude spectra (Fig. 15). At the Pech Merle Cave (solid blue curve in Fig. 15), the spectral amplitude is the smallest of the four sites, smaller than 10^{-4} °C for frequencies larger than 10^{-5} Hz, and the S2 peak, characteristic of APV, is almost completely removed. In the other caves, some peaks do remain in the

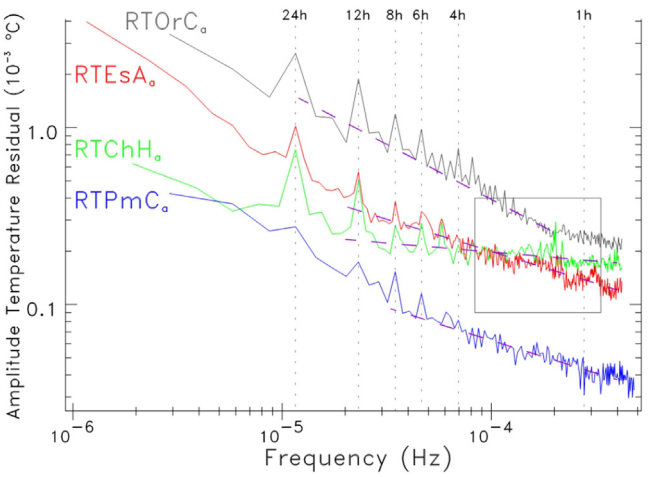

Fig. 15. Amplitude spectra of air temperature residuals versus frequency at Esparros (in red), Pech Merle (in blue), Chauvet (in green) and Aven d'Orgnac Caves (in grey). Independent spectra are stacked to reduce continuum fluctuations. Different time-series are used: time-series from 2005 to 2008 for the Esparros Cave, time-series from 1998 to 1999 for the Aven d'Orgnac Cave, and time-series from 2015 to 2018 for the Pech Merle and Chauvet Caves.

amplitude spectrum of the residuals, but the barometric S2 does not dominate anymore. The remaining peaks are probably due to the S1 peak and its harmonics, which suggests the presence of some diurnal thermal forcing. While this may be expected in Aven d'Orgnac and Esparros Caves, because of the daily cycle in the visits and associated air currents, it is more surprising in the Chauvet Cave. Natural daily effects are mostly diurnal air currents and barometric winds, as diurnal surface temperature variations are too small to be observed at the depth of the cavities by heat diffusion only. Diurnal effects in the Chauvet Cave could proceed through the permeable debris cone which obstructed the natural entrance and should not be air-tight (Bourges et al., 2020). An enhanced diurnal effect due to direct exposure to the sun of the rock scarp overlying the entrance of the cave cannot be ruled out.

In addition to the peaks, the dominating common feature of the amplitude of the residuals is the scale-free nature of the spectra (Fig. 15), which obeys a fractal power-law of the form $f^{-\alpha}$ for frequencies larger than 10^{-5} Hz, over more than one order of magnitude of frequency. When performing a fit of the amplitude spectra, removing the peaks, over the frequency range indicated in Fig. 15 (dashed lines), the following values of α are obtained: -0.103 ± 0.006 for the Chauvet Cave, -0.363 ± 0.003 for the Esparros Cave, -0.370 ± 0.008 for the Pech Merle Cave, and -0.62 ± 0.01 for the Aven d'Orgnac Cave. While the power spectrum at the Chauvet Cave is almost constant, the other caves show a value of the exponent typical of pink noise (referred to sometimes as flicker noise), characterized by an amplitude spectrum of the form $f^{-1/2}$ (Turcotte, 1992). Significant differences, about a factor of 10, emerge on the amplitude values between the various sites. The amplitude spectrum of the residuals for frequencies larger than 8×10^{-5} Hz, therefore, provides a fine thermodynamic assessment of each site. Using this criterion, the most thermodynamically confined site is the Red Corridor in the Pech Merle Cave. The Aragonite Gallery in the Esparros Cave and the Hillaire Room in the Chauvet Cave are similar, but with a factor of about 8 less stable than the Red Corridor of the Pech Merle Cave. However, at high frequency, the residual levels are probably constrained by the instrumental noise. Unlike the other locations (EsA, ChH and OrC in Fig. 15), where the measurements are performed using Pt100 sensors (Perrier et al., this issue), the PmC sensor is a more sensitive SB recorder.

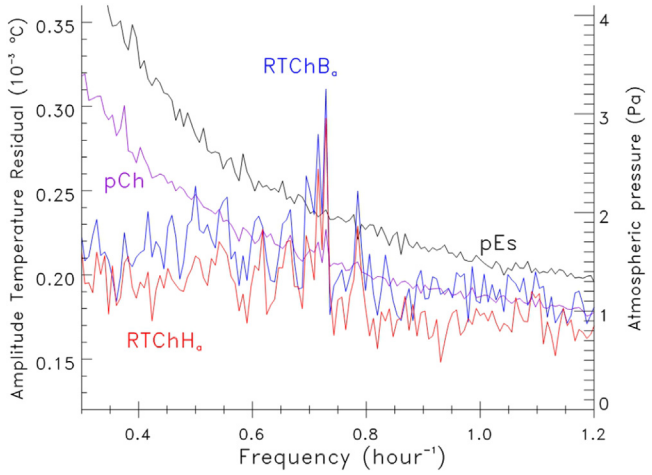

Fig. 16. Amplitude spectrum of air temperature residuals versus frequency, expressed in h^{-1}, at the Chauvet Cave in the Hillaire ($RTChH_a$ in red) and Brunel ($RTChB_a$ in blue) Rooms. The amplitude spectra of atmospheric pressure simultaneously recorded in the Chauvet Cave (in purple) and in the Esparros Cave (in black) are shown with the scale given on the right-hand side. Independent spectra are stacked to reduce continuum fluctuations. A time-series from February 2016 to December 2017 is used.

At the Chauvet Cave, in addition to the harmonics of the S1 wave and the scale-free thermal background, another peak appears in the amplitude spectrum (solid green curve in Fig. 15). This peak emerges more distinctly when enlarging the high-frequency region (Fig. 16), with the dominating peak having a frequency of 0.73 h^{-1} or a period of 1.37 h (82 min or 2×10^{-4} Hz), sufficiently below the Nyquist cut-off frequency for a sampling interval of 15 minutes. This peak, observed both in the Brunel ($RTChB_a$) and Hillaire Rooms ($RTChH_a$), is weakly observed in the amplitude spectrum of the atmospheric pressure (green curve in Fig. 16) recorded in the Bauges Room (Fig. 1c,d). The peak does not appear at all using the atmospheric pressure time-series recorded simultaneously in the Esparros Cave (black curve in Fig. 16). The peak remains when the number of data points used for stacking the amplitude spectra is varied, and can therefore be considered reliable. Other peaks may be present in Fig. 16, but less convincingly. The dominating peak is observed in the time section used in Figs. 15 and 16 (February, 2016 to December, 2017), but was not observed at other times, for example from February to December, 2018.

This weak but definite resonance in the Chauvet Cave is not straightforward to explain. A tentative explanation would be a Helmholtz resonance (Rocard, 1971; Bérest and Habib, 1983; Badino and Chignola, 2019), which involves both temperature and atmospheric pressure. The fundamental Helmholtz frequency for a cavity of volume V, with an access conduit of surface area S and length L is $V_s\sqrt{S/(LV)}/2\pi$, where V_s is the sound velocity in air (Rocard, 1971). However, taking $S = 0.8$ m^2, $L = 20$ m, and for V an extreme upper estimate of 100,000 m^3, we get about 3×10^{-2} Hz, which is inconsistent with the observed resonance at 2×10^{-4} Hz. When taking instead $S = 0.8$ m^2 for the area of the open slit under the door and $L = 7$ m for the access tunnel to the Brunel Room, the resonance frequency becomes 1.4×10^{-2} Hz, which is still too large. The involved air volume is poorly known, but changing the value of the volume involved does not change sufficiently the value of the resonance frequency. Alternatively, if the resonance occurs through a fracture leading to the surface, then we can take $L = 50$ m and $S = 10^{-4}$ m^2, corresponding to a rectangular fracture of width 100 μm and lateral extension 1 m. In that case, the Helmholtz frequency is 2×10^{-4} Hz, assuming that the Helmholtz mechanism and the above equation are still valid for such a narrow conduit. Such a fracture would not be available for air transport when water infiltration massively invades the permeable fractures of the unsaturated zone above the cave, which was the case during the year 2018 during which heavy rainfall occurred after three years of relative drought (Bourges et al., 2020). Thus, while uncertainties remain about the geometry of the involved channels, the observed peak can be tentatively interpreted as an unusual Helmholtz resonance of the cavity, which can be active or extinct, depending on the level of water saturation in the fractures.

5. Conclusions

In this study, we have first used high-quality temperature time-series recorded in four caves of the South of France to assess in details the PIT variations, both in the cave air and at the rock surface (Perrier et al., this issue). After the PIT TFs were precisely characterized, the purpose of the present contribution was then to perform the subtraction (PITS) of these PIT variations and to examine temperature residuals both in the atmosphere and at the rock surface.

After PITS, thermal signatures of human presence are detected unambiguously at all sites, including the associated multi-phase relaxation process. Because of the long (larger than several days) thermal recovery time of underground cavity, cumulative heating appears in the residuals when the visits are too frequent, which may be a potential problem in the caves hosting fragile prehistoric paintings, such as Pech Merle and Chauvet Caves. In addition, in the case of natural caves, the thermal effects of visits cannot be described using a simple box-filling model based on thermal stratification. Pending a better theoretical framework able to account for the heating response to scattered sources and the subsequent relaxation, temperature residuals after PITS are validated as an essential, possibly mandatory, preservation tool. Then, having this tool in hand, controlled heating experiments, similar to the experiments performed in the Vincennes Quarry (Crouzeix et al., 2003, 2006a, 2006b), are needed to develop a better model of the effect of heat sources in natural caves.

Numerous natural processes are revealed by the residuals, with signals that are generally small, of the order of 1 to 10×10^{-3} °C, even if occasionally larger than 40×10^{-3} °C. Such non-random signals cannot be attributed to instrumental noise, evaluated with a standard deviation ranging from 10^{-4} °C to 10^{-3} °C, depending on the type of sensor. Most of the time, processes in the atmosphere dominate, but transient processes involving the rock mass, such as infiltration, water films or condensation-evaporation episodes, can be suspected. In most cases, the source of the signals, however, remains only tentative and will need to be examined more precisely in the future. The variability of the possible processes, however, is a definite result of the present work.

These signals deserved to be unveiled carefully. They are concrete examples of the concept of “trace signals”, proposed by Alain Mangin in the early nineties (Mangin and D'Hulst, 1996), which are small signals having tremendous importance to understand the stability and resilience modes of a precious albeit fragile underground system. To detect such signals, our study illustrates the requirement, also stated decades ago (Mangin and D'Hulst, 1996), that temperature measurements have to be performed with sufficient accuracy, with a sampling interval of 15 minutes or smaller, and over durations of several years to evaluate the effect of seasonal conditions (Mangin and D'Hulst, 1996). Such signals may not only be meaningful for preservation issues in caves (Bourges et al., 2014a), including biological contamination issues (Martin-Sanchez et al. 2012, 2014; Bercea et al., 2019), but also to understand speleothem growth in relation to climate change (Genty, 2008; Genty and Deflandre, 1998), to evaluate

anomalies of microclimate in heritage sites (e.g., Camuffo et al., 2002; Bonacina et al., 2015), or to eliminate artefact signals in underground geophysical observatories (e.g., Trique et al., 1999; Perrier et al., 2004a; Florea et al., 2021) and in underground physics experiments (Bettini, 2014)

To improve our understanding on the origin of processes, it will be necessary to involve other sets of observations, such as acoustic measurements (microbarographs) or differential pressure (Richon et al., 2005, 2009). Long-period seismic measurements may be interesting to study the high-frequency part of the residuals, when temperature is recorded with a sampling interval of 2 minutes or smaller. To constrain the air currents, which may show complex spatial structure, the use of tracers such as radon-222 (*e.g.*, Wilkening and Watkins, 1976; Perrier et al., 2004b; Bourges et al., 2020) and complementary information from particle counters to monitor aerosols (Dredge et al., 2013) will be relevant. Dedicated auxiliary tracing experiments to assess the spatial structure of air currents (Wilkening and Watkins, 1976) will probably become essential tools in the future.

The features that we have concretely established in the four investigated natural caves for the PIT variations, here and in the companion paper (Perrier et al., this issue), offer a generic approach of coupled processes in natural sites. Coupled processes are intrinsic features of such geosystems, characterized by out-of-equilibrium thermodynamic states (Perrier and Le Mouël, 2016). In the companion paper, we have shown that the coupling is not just a correlation function, but that it is valuable to interpret the stationary TFs with a physical model. Here, we have shown that, in a second step, we learn more about the coupled PIT process by studying the residuals. While the residuals uncover other underlying processes, they include possible remnants of the PIT variations. Indeed, the absence of mean coherence with APV does not necessarily prove that transient PIT variations are not possible. In some instances, during particular time periods, residual variations do not seem to be independent of the APV. Transient states are possible, including for example transient barometric currents, which cannot be captured by stationary TFs. Such transient states of the couplings are an inherent feature of the dynamics taking place in natural sites, and may be an intrinsic limitation in the subtraction of coupled processes. The subtraction of PIT, thus, is not as trivial as it could have been anticipated; the interpretation of the residuals, therefore, should always remain cautious.

In the case of the Chauvet Cave, the residuals show a resonant peak. This peak is not systematically observed, but appears for a period at least larger than one year. The appearance of resonances in the context of underground cavities is not completely surprising (Bérest and Habib, 1983; Badino and Chignola, 2019), but the observed frequency, of the order of 2×10^{-4} Hz, is not straightforward to interpret as a Helmholtz resonance, suggesting important limitations in our understanding of the system. It is possible that even an elementary description of such systems requires active connections between an underground cavity and the surface.

Definitely, underground cavities, even at a depth larger than 50 m and more than 200 m away from the entrance, are not dull environments, but exhibit, after PITS, a novel and fascinating realm of stationary and transient signals which are the thermal signatures of specific processes. These signals, signatures of the underlying competing processes, give important insights into the functioning modes and the thermodynamic states of cavities, opening the way to evaluating their possible resistance or resilience against transient or gradual perturbations, such as climate change. They may offer a rare possibility to study whether the response of a natural site to small perturbations provides an assessment of its reaction to a large change, with possible bifurcations between irreversible damage or adaptation, a question which may become one of the most pressing issues of the coming decades.

Author statement

First author designed the study, did the analysis and wrote the paper. François Bourges coordinated since 1995 all experiments in the four caves and prepared the time-series. Dominique Genty and Bruno Lartiges coordinated the scientific programs in Chauvet and Esparros caves, respectively. Jean-Louis Le Mouël developed the theoretical models with the first author since 1999 and supervised the interpretation of heating experiments. Frédéric Girault and Rémi Losno participated in the experiments, in the installation and recovery of temporary sensors, and suggested current developments. Stéphane Bonnet participated in the geological analysis and carried out the 3D topographic surveys. All co-authors contributed in the interpretations and their refinements, edited and corrected the manuscript's text and figures.

Declaration of Competing Interest

The authors declare that they have no known competing financial interests or personal relationships that could have appeared to influence the work reported in this paper.

Acknowledgments

This work contributes to the IdEx Université de Paris *ANR-18-IDEX-0001*. The authors express their gratitude to Joël Ughetto and Stéphane Tocino at the Aven d'Orgnac Cave, to Dominique Baffier, Marie Bardisa, Charles Chauveau, Paulo Rodrigues and the scientific team coordinated by Carole Fritz at the Chauvet Cave, to Bertrand Defois and the late Jean-Luc Zimmermann at the Pech Merle Cave, and to Francis Ferran, Danielle Forgue and Federica Hanrard at the Esparros Cave. The speleological team (Jean-Pierre Bermond-Gonnet, Josiane Dassain and Adrien Lorentz) is thanked for their highly technical assistance to access the remote parts of the Esparros Cave. François Bourges thanks Eric Mauduit and Pascal Foucher at the DRAC Occitanie Services and the members of Laboratoire de Recherche sur les Monuments Historiques from the French Ministry of Culture for their support over the years. Patrick Richon from CEA/DASE is thanked for the Seabird^{TM} SB39+ sensors used in this study. The original version of this manuscript was improved thanks to the careful and informed work of the Associate Editor Andrea Festa and one anonymous reviewer. This work is GIS-GEMS contribution number 2.

Supplementary materials

Supplementary material associated with this article can be found, in the online version, at doi:10.1016/j.geogeo.2022.100146.

References

Badino, G., 2004. Cave temperatures and global climatic change. Int. J. Speleol. 33, 103–114.
Badino, G., Chignola, R., 2019. Fluctuations of atmospheric pressure and the sound of underground karst systems: The Antro del Corchia (Apuane Alps, Italy). Front. Earth Sci. 7, 147.
Beltrami, H., Ferguson, G., Harris, R.N., 2005. Long-term tracking of climate change by underground temperatures. Geophys. Res. Lett. 32, L19707.
Bercea, S., Năstase-Bucur, R., Teodora Moldovan, O., Kenesz, M., Constantin, S., 2019. Yearly microbial cycle of human exposed surfaces in show caves. Subterr. Biol. 31, 1–14.
Bettini, A., 2014. New underground laboratories: Europe, Asia and the. Americas. Phys. Dark Universe 4, 36–40.
Bérest, P., Habib, P., 1983. Détermination du volume d'une cavité souterraine par mesure d'une période d'oscillation. C. R. Acad. Sci. Paris 296, 301–304.
Bonacina, C., Baggio, P., Cappelletti, F., Romagnoni, P., Stevan, A.G., 2015. The Scrovegni Chapel: The results of over 20 years of indoor climate monitoring. Energy Buildings 95, 144–152.
Bourges, F., Genthon, O., Mangin, A., D'Hulst, D., 2006. Microclimate of l'Aven d'Orgnac and other French limestone caves (Chauvet, Esparros, Marsoulas). Int. J. Climatol. 26, 1651–1670.

Bourges, F., Genthon, P., Genty, D., Lorblanchet, M., Mauduit, E., D'Hulst, D., 2014a. Conservation of prehistoric caves and stability of their inner climate: Lessons from Chauvet and other French caves. Sci. Total Environ. 493, 79–91.
Bourges, F., Genty, D., Perrier, F., Lartiges, B., Régnier, E., François, A., Leplat, J., Touron, S., Bousta, F., Massault, M., Delmotte, M., Dumoulin, J.-P., Girault, F., Ramonet, M., Chauveau, C., Rodrigues, P., 2020. Hydrogeological control on carbon dioxide input into the Chauvet-Pont d'Arc cave. Sci. Total Environ. 716, 136844.
Bourges, F., Mangin, A., D'Hulst, D., 2001. Carbon dioxide in karst cavity atmosphere dynamics: the example of the Aven d'Orgnac (Ardèche). C. R. Acad. Sci. Paris 333, 685–692.
Bourges, F., Mangin, A., Genthon, P., Genty, D., D'Hulst, D., Mauduit, E., 2014b. Conservation and handling of decorated prehistoric caves: lessons from environmental monitoring at Chauvet-Pont d'Arc cave. Paleo Special Issue 339–345.
Camuffo, D., Bernardi, A., Sturar, G., Valentino, A., 2002. The microclimate inside the Pollaiolo and Botticelli rooms in the Uffizi Gallery. Florence. J. Cultural Heritage 3, 155–161.
Cañaveras, J.C., Hoyos, M., Sanchez-Moral, S., Sanz-Rubio, E., Bedoya, J., Soler, V., Groth, I., Schumann, P., 1999. Microbial communities associated with hydromagnesite and need-fiber aragonite deposits in a karstic cave (Altamira, Northern Spain). Geomicrobiol. J. 16, 9–25.
Clottes, J., Chauvet, J.-M., Brunel-Deschamps, E., Hillaire, C., Daugas, J.-P., Arnold, M., Cachier, H., Evin, J., Fortin, P., Oberlin, C., Tisnerat, N., Valladas, H., 1995. Les peintures paléolithiques de la grotte Chauvet-Pont d'Arc, à Vallon-Pont d'Arc (Ardèche, France): datations directes et indirectes par la méthode du radiocarbone. C. R. Acad. Sci. 1133–1140 Paris IIA.
Crouzeix, C., Le Mouël, J.-L., Perrier, F., Richon, P., 2006a. Non-adiabatic boundaries and thermal stratification in a confined volume. Int. J. Heat Mass Transf. 49, 1974–1980.
Crouzeix, C., Le Mouël, J.-L., Perrier, F., Richon, P., 2006b. Thermal stratification induced by heating in a non-adiabatic context. Build. Environ. 41, 926–939.
Crouzeix, C., Le Mouël, J.-L., Perrier, F., Richon, P., Morat, P., 2003. Long term thermal evolution and effect of low power heating in an underground quarry. C. R. Geosci. 335, 345–354.
Crouzeix, C., Le Mouël, J.-L., Perrier, F., Shnirman, M.G., Blanter, E., 2006c. Long-term persistence of the spatial organization of temperature fluctuation lifetime in turbulent air avalanches. Phys. Rev. E 74, 036308.
De Freitas, C.R., Littlejohn, R.N., Clarkson, T.S., Kristament, I.S., 1982. Cave climate : assessment of airflow and ventilation. J. Clim. 2, 383–397.
Denis, A., Lastennet, R., Huneau, F., Malaurent, P., 2005. Identification of functional relationships between atmospheric pressure and CO_2 in the cave of Lascaux using the concept of entropy of curves. Geophys. Res. Lett. 32, L05810.
Dominguez-Villar, D., Lojen, S., Krklec, K., Baker, A., Fairchild, I.J., 2015. Is global warming affecting cave temperatures? Experimental and model data from a paradigmatic case study. Clim. Dyn. 45, 569–581.
Drăguşin, V., Tîrlă, L., Cadicheanu, N., Ersek, V., Mirea, I.-C., 2018. Caves as observatories for atmosphere thermal tides: an example from Ascunsă Cave. Romania. Int. J. Speleol. 47, 113–117.
Dredge, J., Fairchild, I.J., Harrison, R.M., Fernandez-Cortes, A., Sanchez-Moral, S., Jurado, V., Gunn, J., Smith, A., Spötl, C., Mattey, D., Wynn, P.M., Grassineau, N., 2013. Cave aerosols: distribution and contribution to speleothem geochemistry. Quat. Sci. Rev. 63, 23–41.
Fernandez, P.L., Gutierrez, I., Quindos, L.S., Soto, J., Villar, E., 1986. Natural ventilation of the Paintings Room in the Altamira cave. Nature 321, 586–588.
Fernandez-Cortes, A., Cuezva, S., Sanchez-Moral, S., Cañaveras, J.C., Porca, E., Jurado, V., Martin-Sanchez, P.M., Saiz-Jimenez, C., 2011. Detection of human-induced environmental disturbances in a show cave. Environ. Sci. Pollut. Res. 18, 1037–1045.
Florea, L.J., Pflitsch, A., Cartaya, E., Stenner, C., 2021. Microclimates in Fumarole Ice Caves on volcanic edifices – Mont Tainier, Washington, USA. J. Geophys. Res. Atmos. 126 e2020JD033565.
Genty, D., 2008. Palaeoclimate research in Villars Cave (Dordogne, SW-France). Int. J. Speleol. 37, 173–191.
Genty, D., Deflandre, G., 1998. Drip flow variations under a stalactite of the Père Noël cave (Belgium). Evidence of seasonal variations and air pressure constraints. J. Hydrol. 211, 208–232.
Houillon, N., Lastennet, R., Denis, A., Malaurent, P., Minvielle, S., Peyraube, N., 2017. Assessing cave internal aerology in understanding carbon dioxide (CO_2) dynamics: Implications on calcite mass variation on the wall of Lascaux Cave (France). Environ. Earth Sci. 76, 170.
Hoyos, M., Soler, V., Cañaveras, J.C., Sanchez-Moral, S., Sanz-Rubio, E., 1998. Microclimatic characterization of a karstic cave: human impact on microenvironmental parameters of a prehistoric rock art cave (Candamo Cave, northern Spain). Environ. Geol. 33 (4), 231–242.
Hunt, G.R., Cooper, P., Linden, P.F., 2001. Thermal stratification produced by plumes and jets in enclosed spaces. Build. Environ. 36, 871–882.
Le Mouël, J.-L., Kossobokov, V., Perrier, F., Morat, P., 2016. Intermittent heat instabilities in an air plume. Non-Linear Process. Geophys 23, 319–330.
Linden, P.F., 1999. The fluid mechanics of natural ventilation. Annu. Rev. Fluid Mech. 31, 201–238.
Linden, P.F., Lane-Serff, G.F., Smeed, D.A., 1990. Emptying filling boxes : the fluid mechanics of natural ventilation. J. Fluid Mech. 212, 309–335.
Lorblanchet, M., 2010. Art pariétal: Grottes ornées du Quercy. Editions du Rouergue, Rodez. In French.
Luetscher, M., Lismonde, B., Jeannin, P.-Y., 2008. Heat exchanges in the heterothermic zone of a karst system: Monlesi case, Swiss Jura Mountains. J. Geophys. Res. 113, F02025.
Mangin, A., D'Hulst, D., 1996. Fréquentation des grottes touristiques et conservation, Méthode d'approche pour en étudier les effets et proposer une règlementation. International Symposium Show Caves and Environmental Monitoring, Cueno, Italy, 1995. A.A. Cigna (Ed.), 137–167.
Mangin, A., Bourges, F., d'Hulst, D., 1999. Painted caves conservation: A stability problem in a natural system (the example of the prehistoric cave of Gargas, French Pyrenees). C. R. Acad. Sci. Paris 328, 295–301.
Martin-Sanchez, P.M., Nováková, A., Bastian, F., Alabouvette, C., Saiz-Jimenez, C., 2012. Two new species of the genus Ochroconis, O. Lascauxensis and O. anomala isolated from black stains in Lascaux Cave, France. Fungal Biol 116, 574–589.
Martin-Sanchez, P.M., Jurado, V., Porca, E., Bastian, F., Lacanette, D., Alabouvette, C., Saiz-Jimenez, C., 2014. Airborne microorganisms in Lascaux Cave (France). Int. J. Speleol. 43, 295–303.
Mejía-Ortiz, L., Christman, M.C., Pipan, T., Culver, D.C., 2020. What's the temperature in tropical caves? Plos One 15, e0237051.
Morat, P., Le Mouël, J.-L., Poirier, J.-P., Kossobokov, V., 1999. Heat and water transport by oscillatory convection in an underground cavity. C. R. Acad. Sci. Paris 328, 1–8.
Morat, P., Le Mouël, J.-L., Pride, S., Jaupart, C., 1995. Remarkable oscillations of temperature, humidity and electric potential observed in an underground quarry. C. R. Acad. Sci. Paris 320, 173–180.
Perrier, F., Bourges, F., Girault, F., Le Mouël, J.-L., Genty, D., Lartiges, B., Losno, R., Bonnet, S. Temperature variations in caves induced by atmospheric pressure variations, 1: Transfer functions and their interpretation. Geosys. Geoenviron. This issue.
Perrier, F., Le Mouël, J.-L., 2016. Stationary and transient thermal states of barometric pumping in the access pit of an underground quarry. Sci. Total Environ. 550, 1044–1056.
Perrier, F., Le Mouël, J.-L., Poirier, J.-P., Shnirman, M.G., 2005. Long-term climate change and surface versus underground temperature measurements in Paris. Int. J. Climatol. 25, 1619–1631.
Perrier, F., Le Mouël, J.-L., Richon, P., 2010. Spatial and temporal dependence of temperature variations induced by atmospheric pressure variations in shallow underground cavities. Pure Appl. Geophys. 167, 253–276.
Perrier, F., Morat, P., Le Mouël, J.-L., 2001. Pressure induced temperature variations in an underground quarry. Earth Planet. Sci. Lett. 191, 145–156.
Perrier, F., Morat, P., Yoshino, T., Sano, O., Utada, H., Gensane, O., Le Mouël, J.-L., 2004a. Seasonal thermal signatures of heat transfer by water exchange in an underground vault. Geophys. J. Int. 158, 372–384.
Perrier, F., Richon, P., Crouzeix, C., Morat, P., Le Mouël, J.-L., 2004b. Radon-222 signatures of natural ventilation regimes in an underground quarry. J. Environ. Radioact. 71, 17–32.
Peyraube, N., Lastennet, R., Denis, A., Malaurent, P., Houillon, N., Villanueva, J.C., 2018. Determination and quantification of major climatic parameters influencing the CO_2 of Lascaux Cave. Theor. Appl. Climatol. 133, 1291–1301.
Rau, G.C., Cuthberg, M.O., Andersen, M.S., Baker, A., Rutlidge, H., Markowska, M., Roshan, H., Marjo, C.E., Graham, P.W., Acworth, R.I., 2015. Controls on cave drip water temperature and implications for speleothem-based paleoclimate reconstructions. Quat. Sci. Rev. 127, 19–36.
Richon, P., Perrier, F., Pili, E., Sabroux, J.-C., 2009. Detectability and significance of 12 hr barometric tide in radon-222 signal, dripwater flow rate, air temperature and carbon dioxide concentration in an underground tunnel. Geophys. J. Int. 176, 683–694.
Richon, P., Perrier, F., Sabroux, J.-C., Trique, M., Ferry, C., Voisin, V., Pili, E., 2005. Spatial and time variations of radon-222 concentration in the atmosphere of a dead-end horizontal tunnel. J. Env. Radioact. 78, 179–198.
Rocard, Y., 1971. Dynamique générale des vibrations. Masson, Paris. In French.
Saiz-Jimenez, C., Cuezva, S., Jurado, V., Fernandza-Cortes, A., Pora, E., Benavente, D., Cañaveras, J.C., Sanchez-Moral, S., 2011. Paleolithic art in peril: Policy and science collide at Altamira cave. Science 334, 42–43.
Šebela, S., Turk, J., 2011. Local characteristics of Postojna Cave climate, air temperature, and pressure monitoring. Theor. Appl. Climatol. 105, 371–386.
Sondag, F., van Ruymbeke, M., Soubiès, F., Santos, R., Somerhausen, A., Seidel, A., Boggiani, P., 2003. Monitoring present day climatic conditions in tropical caves using an Environmental Data Acquisition System (EDAS). J. Hydrol. 273, 103–118.
Trique, M., Richon, P., Perrier, F., Avouac, J.-P., Sabroux, J.-C., 1999. Radon emanation and electric potential variations associated with transient deformation near reservoir lakes. Nature 399, 137–141.
Turcotte, D.L., 1992. Fractals and chaos in geology and geophysics. Cambridge University Press, New York.
Villar, E., Bonet, A., Diaz-Caneja, B., Fernandez, P.L., Gutierrez, I., Quindos, L.S., Solana, J.R., Soto, J., 1984. Ambient temperature variations in the hall of paintings of Altamira cave due to the presence of visitors. Cave Sci. 11, 99–104.
Wilkening, M.H., Watkins, D.E., 1976. Air exchange and ^{222}Rn concentrations in the Carlsbad caverns. Health Phys. 31, 139–145.